Spectral Properties of Tm^{3+}-Doped Silica Glasses and Laser Behaviors of Fibers by Sol-Gel Technology

Li Zhilan[1,2] Wang Shikai[1,2] Wang Xin[1,2] Guan Peiwen[1,2] Li Wentao[1,2] Wang Meng[1]
Yu Chunlei[1] Zhang Lei[1] Li Kefeng[1] Chen Danping[1] Hu Lili[1]

([1] *Shanghai Institute of Optics and Fine Mechanics, Chinese Academy of Sciences, Shanghai* 201800, *China*
[2] *University of Chinese Academy of Sciences, Beijing* 100049, *China*)

Abstract Tm^{3+}-doped silica glasses with molar fraction composition of $0.3Tm_2O_3$-$0.3xAl_2O_3$-$(100-0.3-0.3x)SiO_2$ (x=8, 10, 15, 20) denoted as ATS glasses are prepared by sol-gel method. The spectroscopic properties of the bulk glasses are investigated. The maximum emission cross section and measured fluorescence lifetime at 1811 nm are 6.39×10^{-21} cm^2 and 645 μs, respectively. The lowest OH content is 10.5×10^{-6}. The fiber preform was prepared by rod-in-tube method. The glass with composition $0.3Tm_2O_3$-$4.5Al_2O_3$-$95.2SiO_2$ is used as fiber core; the inner cladding is pure silica glass with an octagonal shape; and the outer cladding is ultraviolet curing layer. Laser properties of the fiber are investigated. The maximum laser output power reaches 1.23 W from a 66-cm-long fiber and the slope efficiency is 11.7%. The lasing threshold is 6.07 W and the lasing wavelength is centered at 1952 nm.

Key words materials; thulium-doped silica fiber; sol-gel method; 2 μm laser
OCIS codes 160.2290; 160.3380; 160.5690

溶胶凝胶法制备的掺铥石英玻璃光谱性质及光纤激光性能

李志兰[1,2] 王世凯[1,2] 王 欣[1,2] 关珮雯[1,2] 李文涛[1,2]
王 孟[1] 于春雷[1] 张 磊[1] 李科峰[1] 陈丹平[1] 胡丽丽[1]

([1]中国科学院上海光学精密机械研究所, 上海 201800
[2]中国科学院大学, 北京 100049)

摘要 用溶胶凝胶法制备了摩尔百分比为 $0.3Tm_2O_3$-$0.3xAl_2O_3$-$(100-0.3-0.3x)SiO_2$(x=8, 10, 15, 20)的一系列铥掺杂石英(ATS)玻璃。研究了样品的光谱性质,1811nm 处最大发射截面为 6.39×10^{-21} cm^2,最长荧光寿命为 645 μs。样品的最低 OH 含量为 10.5×10^{-6}。采用管棒法制备了光纤预制棒,采用组分为 $0.3Tm_2O_3$-$4.5Al_2O_3$-$95.2SiO_2$的玻璃作为纤芯,八边形的纯石英管作为内包层,用紫外固化剂作为外包层拉制双包层光纤。测量了光纤的激光性质,在 66 cm 长的光纤中得到了最大为 1.23 W 的激光输出,斜率效率为 11.7%,激光阈值为 6.07W,激光中心波长为 1952 nm。

关键词 材料; 铥掺杂石英光纤; 溶胶凝胶法; 2 μm 激光
中图分类号 TB32.1 **文献标识码** A **doi**: 10.3788/CJL201340.0806003

收稿日期: 2013-03-25; **收到修改稿日期**: 2013-04-02
基金项目: 国家自然科学基金(60937003)

作者简介: 李志兰(1985—),女,硕士研究生,主要从事溶胶凝胶法制备掺铥石英玻璃及光纤等方面的研究。E-mail:zhilanli@163.com
导师简介: 胡丽丽(1963—),女,研究员,博士生导师,主要从事激光玻璃和特种光纤等方面的研究。E-mail: hulili@laserglass.com.cn

1 Introduction

A lot of work has been done over the past several decades on the thulium-doped glasses and fibers[1-3]. Thulium-doped fiber has an intense emission centered around 2 μm and can offer a large tuning range from 1.7 μm to 2.2 μm. Such a wavelength range overlaps the absorption band of water at 1.93 μm and covers the absorption peaks of methane gases and carbon dioxide. These features make 2 μm lasers very useful in applications such as environmental pollution detection, eye safe laser radar, satellite communications, laser remote sensing, especially in high-energy-per-pulse mode, as well as medical area[4-6].

So far, many thulium-doped glasses such as tellurite[7], germanate[8], fluoride[9] and silica glasses[10] have been studied. For fiber laser application, tellurite glass, germanate glass and fluoride glass have low mechanical strength. They are hard to splice with commercial silica fiber. Those problems restrict their practical applications[11]. Rare earth doped silica fiber has many attractive properties such as high ultraviolet (UV) transparency, high mechanical strength and easy to link with commercial silica fibers through fusion splice technique. These characteristics make it widely used in fiber laser devices[12]. From a large number of researches on Tm-doped silica fibers, it has been noted that the laser output power and efficiency of the fiber increase when Tm^{3+} ions are co-doped with appropriate amount of Al^{3+} ions. Al^{3+} ions in silica can reduce the cluster of Tm^{3+} ions and increase the Tm^{3+} doping level. High Tm^{3+} doping level in fiber can reduce the fiber length, thus can decrease the overall fiber loss. Meanwhile, usage of shorter fiber can reduce the nonlinear optical effects. Moreover, higher Tm^{3+} doping level can enhance the cross-relaxation process, which is beneficial to improve the output power and slope efficiency of laser[13-15].

The well-known method of preparing Tm^{3+} doped silica fiber is the modified chemical vapor deposition (MCVD) technique combining with the solution doping[16]. This traditional method has some drawbacks such as the limitation of rare earth doping level and inhomogeneous distribution of rare earth ions. Other techniques of rare earth doped silica preform fabrication such as direct nanoparticle deposition (DND)[17] and sol-gel methods[18] have been developed and reported. The DND technology is a new patented technique for fiber production. It has been proved to be difficult to achieve high level doping of rare earth ions[19]. Sol-gel technique can realize the homogeneity of mixtures and make the doping concentration reach a high level[20]. Liu *et al.*[21] prepared Yb^{3+} doped silica glass using sol-gel method. Artizzu *et al.*[22] investigated the emission properties, energy transfer mechanism, the sensitization efficiency of silica sol-gel glasses incorporating dual-luminescent Yb quinolinolato complex. Silversmith *et al.*[23] studied the fluorescence yield in rare-earth-doped sol-gel silicate glasses. But till now, there is no report on Tm^{3+} doped silica glasses by sol-gel method.

In this work, Tm^{3+}, Al^{3+} co-doped silica glasses with different ratios of Al^{3+}/Tm^{3+} are prepared and the spectroscopic properties of these samples are investigated. A preform with core of Tm^{3+}, Al^{3+} co-doped silica glass and the inner cladding of pure silica glass is fabricated with rod-in-tube method. Fiber is drawn and coated with a low refractive index ultraviolet curing layer as outer cladding. The properties of Tm^{3+}, Al^{3+} co-doped silica glass and laser behaviors of double cladding fiber are studied.

2 Experiments

2.1 Samples preparation

A series of Tm^{3+}, Al^{3+} co-doped silica glasses with molar fraction compositions of $0.3Tm_2O_3$-$0.3xAl_2O_3$-$(100-0.3-0.3x)SiO_2$ (x = 8, 10, 15, 20, corresponding to ATS1, ATS2, ATS3, ATS4) were prepared. Tetraethoxysilane (TEOS), $AlCl_3 \cdot 6H_2O$ and $TmCl_3 \cdot 6H_2O$ were used as the precursors for SiO_2, Al_2O_3 and Tm_2O_3, respectively. Different Al/Tm ratios were used to optimize properties of spectroscopy and glass formation. All reactants were analytically pure. Deionized water, ethanol and ammonia were used as hydrolysis reactant, solvent and catalyzer, respectively. The mixed solution was kept stirring at 45 ℃ for about 3 h in order to obtain homogeneous sol. During this period the hydrolysis reaction occurred[24]. The homogeneous sol was gelled at 80 ℃ and desiccated at 600 ℃ for 3 h to remove organic impurities and adsorbed water. The xerogel was then sintered at 1750 ℃ and transformed into amorphous transparent glasses. The glasses were molded into rod and slice samples by the oxy-hydrogen flame heating. Slice samples were processed into 2 mm thickness for spectroscopic properties tests. The glass rod was ground and polished into proper diameter for the preparation of the preform by rod-in-tube method.

2.2 Characterization of glasses and fiber

The refractive index of glass was measured by

waveguide prism coupling method with thickness of 0.5 mm and the density was tested by Archimedes' liquid-immersion method in distilled water. Tm_2O_3 concentration was measured by inductively coupled plasma atomic emission spectroscopy (ICP-AES). All samples were polished to 2 mm thick for spectroscopic measurements. Absorption spectra were recorded with a Perkin-Elmer-Lambda 900UV/VIS/NIR spectrophotometer in the range of 200 ~ 2000 nm. Emission spectra were measured with a Traix 320 type spectrometer (Jobin-Yvon Co., France) by using a 794 nm laser diode as excitation source. Fourier transform infrared spectroscopy (FTIR) spectra were measured using a spectrophotometer (Nexus FT-IR Spectrometer, Thermo Nicolet). All the measurements were performed at room temperature. Laser experimental setup on fiber will be given in following sections.

3 Results and discussion

3.1 Density and refractive index of glasses

The densities ρ, refractive indices n_d and Tm^{3+} ion concentrations N of glass samples are presented in Table 1. It can be clearly seen that the densities and refractive indices of ATS2 to ATS4 glasses are higher than those of ATS1. They increase with the addition of Al_2O_3. Tm^{3+} ion concentrations in Table 1 are calculated from measured Tm_2O_3 concentration and glass density. It changes from 1.14×10^{20} cm^{-3} to 1.23×10^{20} cm^{-3}, although the mean Tm_2O_3 concentration is 0.3% (molar fraction) in each glass.

Table 1 Densities, refractive indices and Tm^{3+} concentrations of glass samples

Sample	ATS1	ATS2	ATS3	ATS4
ρ / (g/cm^3)	2.22	2.26	2.26	2.27
n_d	1.457	1.461	1.463	1.460
N /(10^{20} cm^{-3})	1.21	1.23	1.15	1.14

3.2 Absorption spectra and Judd-Ofelt analysis

The absorption spectra were obtained over a spectral range of 300~2000 nm. The ATS samples have almost the same absorption intensity and absorption cross section because there is no obvious difference in the Tm^{3+} ion concentrations of samples. The absorption cross section is calculated using the Beer-Lambert equation[25]:

$$\sigma_a(\lambda)=\frac{2.303}{NL}D(\lambda), \tag{1}$$

where N is the rare earth ion concentration, L is the sample thickness, and $D(\lambda)$ is optical density which can be obtained from absorption spectra subtracted by baseline. Figure 1(a) shows the absorption spectra and Fig.1(b) shows the absorption cross sections of the ATS samples calculated according to Eq.(1). There are six bands centered at 354, 470, 687, 793, 1210 and 1670 nm, corresponding to the absorptions from the ground state $^3H_6$ to the excited states $^1D_2$, $^1G_4$, $^3F_{2,3}$, $^3H_4$, $^3H_5$ and $^3F_4$. The transitions to the levels higher than $^1D_2$ are not observed because of the strong intrinsic absorption of the host glass near ultraviolet waveband.

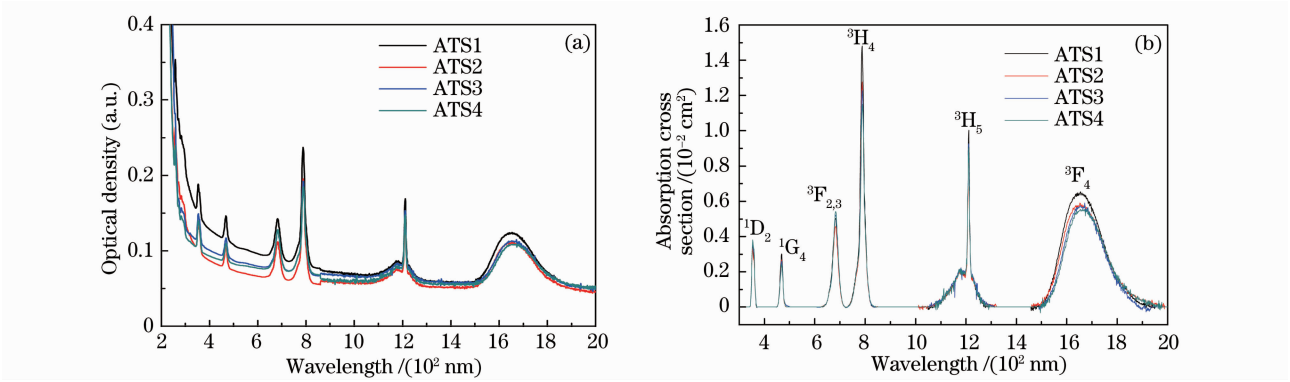

Fig.1 (a) Absorption spectra and (b) absorption cross section of ATS samples

According to Judd-Ofelt (J-O) theory [26-27], five absorption bands ($^1D_2$, $^1G_4$, $^3H_4$, $^3H_5$ and $^3F_4$) together with the density and the refractive index are used to calculate the J-O intensity parameters $\Omega_{2,4,6}$ and the radiative transition rates. Previous study[28] revealed that the Ω_2 parameter is indicative of the amount of the covalent bond and strongly depends on the symmetry of local environments of Tm^{3+} ion sites, while the Ω_6 parameter is related to the overlap integrals of the 4f and 5d orbits of Tm^{3+} ions. Values of Ω_4 and Ω_6 also provide some information on the rigidity and viscosity of hosts. Table 2 lists the J-O intensity parameters of Tm^{3+} and $^3F_4\rightarrow{}^3H_6$ radiative transition rates (A_{rad}) in present work and in other glasses reported in literatures. We can see that the value of Ω_2 for silica glass is much higher than those of bismuthate[29], tellurate[30], germanate[31] and fluoride[9] glasses, which means that the silica glass has stronger asymmetry and polarization, meanwhile, the

bond covalency of Tm－O in silica glass is stronger than those in other glasses. Furthermore, it can be found that the value of Ω_2 decreases with the increase of the Al_2O_3 additive. It means that the surrounding of Tm^{3+} ion in silica glass becomes less asymmetrical with the increase of Al_2O_3. Value of A_{rad} for Tm^{3+} : ${}^3F_4 \rightarrow {}^3H_6$ transitions decreases with the increase of Al_2O_3. A_{rad} is proportional to the electric dipole line strength S_{ed} which has positive correlation with $\Omega_{2,4,6}$, especially with Ω_2. So A_{rad} and Ω_2 have the same variation tendency with the increase of Al_2O_3 concentration.

Table 2　J-O intensity parameters of Tm^{3+} ion in various glasses and ${}^3F_4 - {}^3H_6$ A_{rad} in ATS glasses. The error limit is 5%

Glasses	Ω_2 /(10^{-20} cm^2)	Ω_4 /(10^{-20} cm^2)	Ω_6 /(10^{-20} cm^2)	A_{rad}/s^{-1}	Reference
ATS1 (this work)	8.98	3.29	3.08	278.9	
ATS2 (this work)	8.41	3.21	2.39	262.5	
ATS3 (this work)	6.4	3.43	3.12	237.1	
ATS4 (this work)	6.41	3.62	2.85	238.3	
Bi_2O_3-GeO_2-Na_2O	4.35	1.49	0.96	–	[29]
TWL30	4.48	1.77	1.39	–	[30]
GeO_2-Ga_2O_3-Bi_2O_3-PbO	2.84	0.5	0.75	–	[31]
ZBLAN	1.96	1.36	1.16	–	[9]
Silica	6.23	1.91	1.36	–	[9]

3.3　Fluorescence spectra and stimulated emission cross section

The fluorescence spectra of Tm^{3+}-doped silica glasses pumped at 808 nm with diode laser are shown in Fig. 2(a). It can be seen that there is a strong emission at 1.8 μm and a weak emission at 1.47 μm in the range of 1.3 ～ 2.2 μm, corresponding to the transition of Tm^{3+} : ${}^3F_4 \rightarrow {}^3H_6$ and ${}^3H_4 \rightarrow {}^3F_4$. The low emission intensity of 1.47 μm may be caused by two processes. One is that Tm^{3+} ion at the ${}^3H_4$ level has a non-radiative transition to ${}^3H_5$ level through multi-phonon relaxation process and the other is that the Tm^{3+} ion at the ${}^3H_4$ state transfers its energy to another Tm^{3+} ion at the ground state which is the well-known cross-relaxation process (${}^3H_4 + {}^3H_6 \rightarrow {}^3F_4 + {}^3F_4$). The relative emission intensity ratio of 1.8 μm to 1.47 μm bands can partially reflect the cross-relaxation efficiency. The relative emission intensity ratio of 1.8 μm to 1.47 μm of samples is calculated to be 212, 244, 249 and 199 corresponding to ATS1, ATS2, ATS3 and ATS4. It can be concluded that ATS3 glass with Al^{3+}/Tm^{3+} ratio of 15∶1 has the most efficient cross-relaxation.

The stimulated emission cross section (σ_{emi}) of Tm^{3+} : ${}^3F_4 \rightarrow {}^3H_6$ transition can be calculated according to Fuchbauer-Ladenburg theory[32-33]

$$\sigma_{emi}(\lambda) = \frac{\lambda^4 A_{rad}}{8\pi c n^2} \times \frac{\lambda I(\lambda)}{\int \lambda I(\lambda)\,\mathrm{d}\lambda}, \tag{2}$$

where $I(\lambda)$ is the emission intensity in fluorescence spectrum, n is refractive index, c is light speed, A_{rad} is radiative transition rate. The results are shown in Fig. 2(b). Large $\sigma_{emi} \times \tau$ (τ denotes lifetime) is very important for obtaining high laser gain. It is a significant parameter of laser materials[33]. Table 3 lists the values of maximum emission cross section (σ_{emi}), measured lifetimes (τ_f), and $\sigma_{emi} \times \tau_f$ for Tm^{3+} : ${}^3F_4 \rightarrow {}^3H_6$ transition in ATS glasses. The values of the cross section in the four samples are in good agreement with those reported in literatures[9,34-35]. Quantum efficiency calculated by

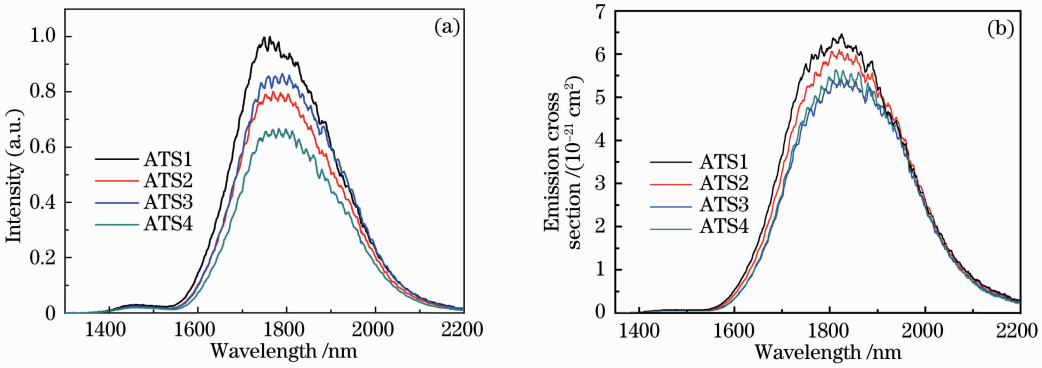

Fig. 2　(a) Emission spectra and (b) emission cross sections of Tm^{3+} ions in ATS glasses

τ_f/τ_{rad} (τ_{rad} denotes radiative lifetime) is listed in Table 3. The maximum emission cross section decreases as Al content increases because of the positive correlation between emission cross section and radiative transition rate as shown in Eq.(2). The measured and calculated lifetimes of $^3F_4$ level increase with increased Al content. The quantum efficiency shows similar variation tendency, that may be caused by the local environment variation of rare earth ions. The rare earth ions are more likely to be connected with Al than Si[14]. The Al－O bond has lower vibration frequency than Si－O bond, so the sample with lower Al content induces higher multi-phonon relaxation rate and shorter lifetime. Tm^{3+} ion in the glasses has the maximum emission cross section of 6.39×10^{-21} cm^2 at 1811 nm in ATS1 glass and the maximum $\sigma_{emi}\times\tau_R$ of 3.50×10^{-21} $cm^2\cdot ms$ in ATS4.

Table 3 Emission cross section at 1.8 μm band and $\sigma_{emi}\times\tau_f$ of Tm^{3+} ion in different glasses

Glasses	σ_{emi} /(10^{-21} cm^2)	τ_f /μs	τ_{rad} /ms	$\sigma_{emi}\times\tau_f$ /(10^{-21} $cm^2\cdot ms$)	η /%
ATS1	6.39	492	3.585	3.14	13.7
ATS2	6.10	522	3.810	3.18	13.7
ATS3	5.40	600	4.218	3.24	14.2
ATS4	5.43	645	4.196	3.50	15.4

The lifetime τ_f is obtained by measurement and others are calculated values. The error limit of values calculated by Judd-Ofelt theory is 5%

3.4 FTIR spectra

The OH groups in glass have strong absorption in near infrared range. They can interact with the rare earth ions, inducing the non-radiative transition in excited state levels. FTIR spectra of ATS glasses are given in Fig.3. The absorption peak of OH in ATS glass is around 3663 cm^{-1}.

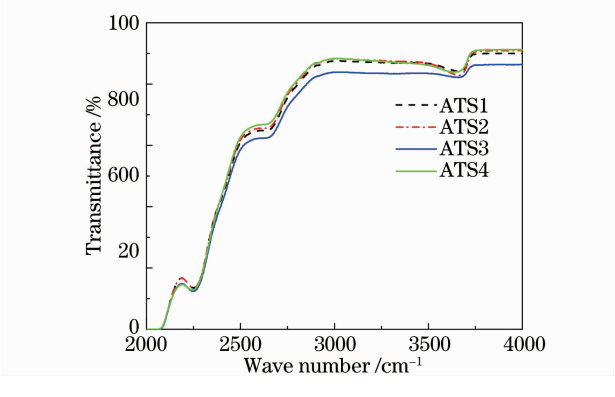

Fig.3 FTIR spectra of 2-mm-thick Tm^{3+}-doped silica glass

Absorption coefficient (α) of OH groups in glass can be calculated by[36]

$$\alpha=\frac{1}{l}\ln\frac{T_0}{T},\tag{3}$$

where l is the sample thickness, T_0 is the baseline transmission of the infrared spectrum, and T is the transmission near 3660 cm^{-1} absorption peak. The OH content can be expressed by[37]

$$C_{OH}=\frac{M_{OH}}{\varepsilon\times\rho}\times\frac{1}{l}\times\ln\frac{T_0}{T},\tag{4}$$

where M_{OH} is the molar weight of OH group, ε is the extinction coefficient and the value of 77.5 $L\cdot mol^{-1}\cdot cm^{-1}$ is used here according to the literature[38], and ρ ($g\cdot cm^{-3}$) is the density of glass sample. The calculated absorption coefficient (α) and OH content (C_{OH}) of sample are listed in Table 4. It is indicated that most of OH groups in the samples have been removed.

Table 4 Absorption coefficients at 3660 cm^{-1} and OH content in glasses

Sample	ATS1	ATS2	ATS3	ATS4
α /cm^{-1}	0.34	0.5	0.25	0.41
$C_{OH}/10^{-6}$	14.7	20.9	10.5	17.3

3.5 Laser performance

The double-cladding Tm^{3+}-doped silica fiber was fabricated by rod-in-tube and drawing method. The core glass composition was $0.3Tm_2O_3$-$4.5Al_2O_3$-$95.2SiO_2$. The fiber had 35 μm core diameter and 280 μm inner cladding diameter. The core numerical aperture (NA) and cladding NA were 0.192 and 0.366, respectively. Figure 4 shows the schematic configuration of the Tm^{3+}-doped double-cladding fiber laser experiment. The pump source was a multimode fiber pigtailed diode laser working around 790 nm. The pump laser was collimated and focused on the Tm-doped silica fibers through a 10× microscope objective. The Tm^{3+}-doped silica fibers were straightly cleaved on both ends. A reflective mirror coated with a dichroic thin film had a high reflectivity (HR, higher than 99.9%) near 1900 nm and high transmissivity (HT) near 800 nm, and it was used as a reflector at the pump end of fiber. The output

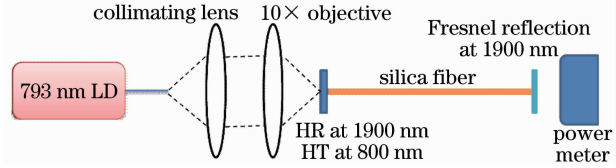

Fig.4 Schematic of the experimental setup of the diode-pumped silica fiber laser

end was with a Fresnel reflection between silica and air of about 3.53%. A long-pass filter was placed before the power meter and spectrometer to attenuate unabsorbed pump light in spectral and power measurements. The about 2 μm laser spectrum of the fiber was measured using a StellarNet RED-Wave NIRx spectrometer.

Figure 5 (a) shows the laser spectrum of the Tm^{3+}-doped silica fiber and the inset is the cross section of the fiber. Figure 5(b) presents the laser output power versus pump power. The fiber length is 66 cm. The lasing wavelength is centered at 1952 nm which is about 160 nm longer than the emission peak in the glass slice in Fig. 2 due to the excited state absorption effect. The background loss measured using cutback method is about 4 dB/m at 1053 nm. The laser threshold is 6.07 W, the maximum laser output power is about 1.23 W and the slope efficiency is 11.7%. The low laser efficiency may be caused by the high loss at present fiber. Further work is being done to reduce the loss and to improve the laser efficiency.

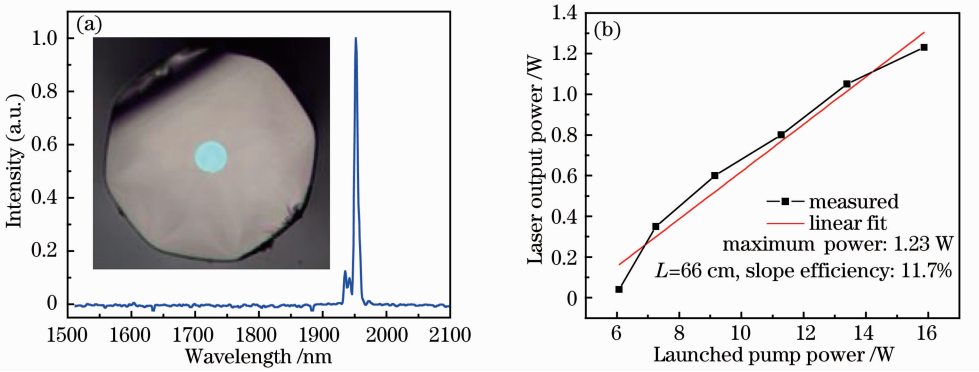

Fig. 5 (a) Laser spectrum of Tm^{3+}-doped silica fiber, the inset is cross section of fiber; (b) laser output power versus pump power

4 Conclusions

Spectroscopic properties of Al^{3+}, Tm^{3+}-codoped silica glasses with different Al/Tm ratios prepared by sol-gel method are investigated. The mean Tm_2O_3 content was kept 0.3% in molar fraction. Both J-O intensity parameter Ω_2 and radiative transition rate A_{rad} decrease with the increase of Al_2O_3 concentration. The maximum emission cross section and measured fluorescence lifetime at 1811 nm are 6.39×10^{-21} cm^2 and 645 μs, respectively. The lowest OH content of 10.5×10^{-6} is achieved. It can be concluded that the glass with Al^{3+}/Tm^{3+} ratio of 15∶1 has the most efficient cross-relaxation. Double-cladding Tm^{3+}-doped silica fiber was fabricated based on the core glass composition of $0.3Tm_2O_3$-$4.5Al_2O_3$-$95.2SiO_2$ and 1.23 W laser output at 1952 nm was obtained. It is for the first time that, to our best knowledge, watt level laser output around 2 μm is realized in Tm^{3+}-doped silica fiber by sol-gel technique. Further work on reducing optical loss is being done.

References

1 D Y Shen, J K Sahu, W A Clarkson. High-power widely tunable Tm∶fibre lasers pumped by an Er, Yb co-doped fibre laser at 1.6 μm [J]. Opt Express, 2006, 14(13): 6084 - 6090.

2 W A Clarkson, N P Barnes, P W Turner, *et al*.. High-power cladding-pumped Tm-doped silica fiber laser with wavelength tuning from 1860 to 2090 nm [J]. Opt Lett, 2002, 27(22): 1989 - 1991.

3 Z S Sacks, Z Schiffer, D David. Long wavelength operation of double-clad Tm∶silica fiber lasers [C]. SPIE, 2007, 6453: 645320.

4 B M Walsh. Review of Tm and Ho materials: spectroscopy and lasers[J]. Laser Phys, 2009,19(4): 855 - 866.

5 M Richardson, L Shah, R A Sims, *et al*.. High power thulium fiber lasers[C]. SPPCom, 2011. SOWD1.

6 T F Morse, K Oh, L J Reinhart. Carbon dioxide detection using a co-doped Tm-Ho optical fiber[C]. SPIE, 1995, 2510: 158 - 164.

7 K Li, G Zhang, L Hu. Watt-level ~2 μm laser output in Tm^{3+}-doped tungsten tellurite glass double-cladding fiber[J]. Opt Lett, 2010, 35(24): 4136 - 4138.

8 J Wu, Z Yao, J Zong, *et al*.. Highly efficient high-power thulium-doped germanate glass fiber laser[J]. Opt Lett, 2007, 32(6): 638 - 640.

9 B M Walsh, N P Barnes. Comparison of Tm∶ZBLAN and Tm∶silica fiber lasers: spectroscopy and tunable pulsed laser operation around 1.9 μm[J]. Appl Phys B, 2004, 78(3 - 4): 325 - 333.

10 G Frith, D G Lancaster, S D Jackson. 85 W Tm^{3+}-doped silica fibre laser[J]. Electron Lett, 2005, 41(12): 687 - 688.

11 H Lin, X Wang, L Lin, *et al*.. Near-infrared emission character of Tm^{3+}-doped heavy metal tellurite glasses for optical amplifiers and 1.8 μm infrared laser[J]. J Phys D: Appl Phys, 2007, 40(12): 3567 - 3572.

12 T Yamamoto, Y Miyajima, T Komukai. 1.9 μm Tm-doped silica fibre laser pumped at 1.57 μm[J]. Electron Lett, 1994, 30(3): 220 - 221.

13 P F Moulton, G A Rines, E V Slobodtchikov, *et al*.. Tm-doped fiber lasers: fundamentals and power scaling [J]. IEEE J Sel Top Quantum Electron, 2009, 15(1): 85 - 92.

14 S D Jackson, S Mossman. Efficiency dependence on the Tm^{3+} and Al^{3+} concentrations for Tm^{3+}-doped silica double-clad fiber lasers[J]. Appl Opt, 2003, 42(15): 2702 - 2707.

15 S D Jackson. Cross relaxation and energy transfer upconversion

processes relevant to the functioning of 2 μm Tm^{3+}-doped silica fibre lasers[J]. Opt Commun, 2004, 230(1-3): 197-203.

16 Wang Wentao, Ruan Ling, Ning Ding, *et al*.. Researches on dopant concentration of a thulium-doped silica fiber[J]. Optical Communication Technology, 2000, (4): 273-276.
王文涛,阮 灵,宁 鼎,等. 掺铥石英光纤的掺杂浓度实验研究[J]. 光通信技术, 2000, (4): 273-276.

17 S Tammela, M Soderfund, J Koponen, *et al*.. The potential of direct nanoparticle deposition for the next generation of optical fibers[C]. SPIE, 2006, 6116: 611616.

18 M C Ferrara, C Blasi. Sol-gel synthesis and characterisation of erbium-modified silica glasses[J]. Mater Lett, 2004, 58(9): 1490-1493.

19 Alain Pastouret, Ekaterina Burov, David Boivin, *et al*.. Amplifying Optical Fiber and Method of Manufacturing[P]. U S Patent, 20100118388, 2010-5-13.

20 A Biswas, J Sahu, H N Acharya. Sol-gel synthesis of Pr-doped silica glasses[J]. Mater Sci Eng B, 1996, 41(3): 329-332.

21 S Liu, H Li, Y Tang, *et al*.. Fabrication and spectroscopic properties of Yb^{3+}-doped silica glasses using the sol-gel method[J]. Chin Opt Lett, 2012, 10(8): 081601

22 F Artizzu, F Quochi, M Saba, *et al*.. Silica sol-gel glasses incorporating dual-luminescent Yb quinolinolato complex: processing, emission and photosensitising properties of the 'antenna' ligand [J]. Dalton Transactions, 2012, 41(42): 13147-13153.

23 A J Silversmith, N T T Nguyen, D L Campbell, *et al*.. Fluorescence yield in rare-earth-doped sol-gel silicate glasses[J]. J Lumin, 2009, 129(12): 1501-1504.

24 Sun Guozhong, Zhao Quanlin, Liu Haitao, *et al*.. Silica glass prepared by sol-gel method[J]. Chemical Industry Times, 1999, (4): 20-22.
孙国忠,赵泉林,刘海涛,等. 溶胶-凝胶法制备 SiO_2 玻璃[J]. 化工时刊, 1999, (4): 20-22.

25 G X Chen, Q Y Zhang, G F Yang, *et al*.. Mid-infrared emission characteristic and energy transfer of Ho^{3+}-doped tellurite glass sensitized by Tm^{3+} [J]. J Fluorescence, 2007, 17(3): 301-307.

26 B Judd. Optical absorption intensities of rare-earth ions[J]. Phys Rev, 1962, 127(3): 750-761.

27 G S Ofelt. Intensities of crystal spectra of rare-earth ions[J]. J Chem Phys, 1962, 37(3): 511-520.

28 J Heo, Y B Shin, J N Jang. Spectroscopic analysis of Tm^{3+} in $PbO-Bi_2O_3-Ga_2O_3$ glass[J]. Appl Opt, 1995, 34(21): 4284-4289.

29 H Fan, G Gao, G Wang, *et al*.. Tm^{3+} doped $Bi_2O_3-GeO_2-Na_2O$ glasses for 1.8 μm fluorescence[J]. Opt Mater, 2010, 32 (5): 5627-631.

30 Li Kefeng, Wang Guonian, Hu Lili, *et al*.. Effects of WO_3 contents on the thermal and spectroscopic properties of Tm^{3+}-doped $TeO_2-WO_3-La_2O_3$ glasses[J]. J Inorganic Materials, 2010, 25(4): 429-434.
李科峰,汪国年,胡丽丽,等. WO_3 含量对 Tm^{3+} 掺杂 $TeO_2-WO_3-La_2O_3$ 玻璃热学性能及光谱性质的影响[J]. 无机材料学报, 2010, 25(4): 429-434.

31 D M Shi, Q Y Zhang, G F Yang, *et al*.. Spectroscopic properties and energy transfer in $Ga_2O_3-Bi_2O_3-PbO-GeO_2$ glasses codoped with Tm^{3+} and Ho^{3+} [J]. J Non-Cryst Solids, 2007, 353(16-17): 1508-1514.

32 S A Payne, L L Chase, L K Smith, *et al*.. Infrared cross-section measurements for crystals doped with Er^{3+}, Tm^{3+}, and Ho^{3+} [J]. IEEE J Quantum Electron, 1992, 28(11): 2619-2630.

33 B Zhou, E Y-B Pun, H Lin, *et al*.. Judd-Ofelt analysis, frequency upconversion, and infrared photoluminescence of Ho^{3+}-doped and Ho^{3+}/Yb^{3+}-codoped lead bismuth gallate oxide glasses[J]. J Appl Phys, 2009, 106(10): 103105.

34 S D Jackson, T A King. Theoretical modeling of Tm-doped silica fiber lasers[J]. J Lightwave Technol, 1999, 17(5): 948-956.

35 X Zou, H Toratani. Spectroscopic properties and energy transfers in Tm^{3+} singly- and Tm^{3+}/Ho^{3+} doubly-doped glasses[J]. J Non-Cryst Solids, 1996,195(1-2): 113-124.

36 D Zhuo, G Qi, B Peng. Determination of water content in phosphate laser glass[J]. Chin Phys Lasers, 1986, 13(3): 212-215.

37 Wang Deping, Huang Wenhai, Zhou Zhihao. Effect of hydroxyl concentration on the properties of commercial soda lime silica glasses[J]. J Building Materials, 1998, 1(4): 375-378.
王德平,黄文海,周志豪. 钠钙硅玻璃中的羟基含量对其性能的影响[J]. 建筑材料学报, 1998, 1(4): 375-378.

38 J Kirchhof, S Unger, A Schwuchow, *et al*.. The influence of Yb^{2+} ions on optical properties and power stability of ytterbium doped laser fibers[C]. SPIE, 2010, 7598: 759801

栏目编辑: 宋梅梅